Cascaded Mode-Locked Nd:YVO_4 Laser Using MgO Doped Periodically-Poled $LiNbO_3$ With Direct In-Band Diode Pumping at 914 nm

Tin-Yu Yang, Yuan-Yao Lin, Shou-Tai Lin, and An-Chung Chiang

***Abstract*—We report a cascaded mode-locked Nd:YVO_4 laser at 1064 nm with direct in-band pumping at 914 nm. A 25-mm-long MgO doped periodically-poled $LiNbO_3$ crystal was used to produce mode-locked laser pulses. A volume Bragg grating was used to manipulate the output spectrum of the laser. In the positive Kerr-lens scheme, the output power was 3.81 W at 166.8-MHz repetition rate. In the negative Kerr-lens scheme, the output power was 4.81 W at 108.6-MHz repetition rate. Typical pulse duration and the full-width-at-half-maximum spectral width were 35 ps and 0.05 nm, respectively, yielding a time-bandwidth product of 0.5.**

***Index Terms*—Lasers, mode-locking, PPLN, volume Bragg grating.**

I. Introduction

KERR-LENS mode-locking (KLM) which utilizes the self-focusing effect due to nonlinear phase distortion in the laser gain medium itself due to intrinsic third order nonlinearity $\chi^{(3)}$, has been demonstrated to be very promising in producing femtosecond laser pulses [1], [2]. Recently, narrow-band picosecond laser pulses are needed for a variety of applications, such as pumping of optical parametric oscillators, nonlinear chirped pulse amplifiers, material processing, and biomedical imaging. However, in picosecond regime, KLM has not been applicable because the picosecond intracavity peak power is insufficient to drive the $\chi^{(3)}$ nonlinear process to obtain enough intracavity loss modulation so as to achieve laser mode-locking. An alternative approach for passive mode locking is nonlinear-mirror (NLM) mode locking, which was proposed by Stankov and Jethwa [3]. The NLM mode locking consists of a nonlinear optical crystal for frequency doubling near a dichroic output coupler, which is highly reflective at the second harmonic wavelength and partially reflective at the fundamental/oscillation wavelength. Fractional back conversion of second harmonic wave (SHW) into fundamental wave (FW) appears once the phase control between two waves is appropriated. When the frequency doubling process is operated in the phase-mismatched regime, the accumulated nonlinear phase of the FW resembles an effective nonlinear index of refraction. Decrease of intra-cavity loss with the generation of FW facilitates the formation of mode-locked laser pulses. The bi-directional frequency doubling process through the nonlinear crystal can be seen as a cascaded second order interaction, also known as cascaded mode-locking (CML), which can result in an effective $\chi^{(3)}$ nonlinearity much larger than the natural third-order nonlinearity in all conventional laser and nonlinear materials [4], [5]. In the non-depleted regime of the frequency doubling process, the effective nonlinear index of refraction can be expressed by [4]

$$\mathrm{n}_2^{\mathrm{eff}} = -\frac{4\pi}{\mathrm{c}\varepsilon_0}\frac{\mathrm{L}}{\lambda}\frac{\mathrm{d}_{\mathrm{eff}}^2}{\mathrm{n}_{2\omega}\mathrm{n}_{\omega}^2}\frac{1}{\Delta k\mathrm{L}}, \tag{1}$$

where ΔkL is the phase-mismatched term in the frequency doubling process, L is the length of the nonlinear crystal, $\mathrm{d}_{\mathrm{eff}}$ is the effective nonlinear coefficient, n_{ω} and $\mathrm{n}_{2\omega}$ are the refractive indices of FW and SHW, respectively, λ is the wavelength of FW, ε_0 is the vacuum permittivity, and c is the speed of light. The magnitude of the effective nonlinear index of refraction can be one order larger than the intrinsic one. The sign of $\mathrm{n}_2{}^{\mathrm{eff}}$, manipulated by ΔkL, determines a positive Kerr lens or a negative one. Both of them can be used to produce mode-locked pulses. NLM mode locking has become the simplest method to produce picosecond laser pulses with a very compact configuration upon use of a suitable laser gain material [6]. The pulse duration of NLM mode-locked pulses, limited by the group velocity mismatching (GVM) between SHW and FW, is usually in the range of picoseconds.

Among the most common solid-state-laser crystals, Nd:YVO_4 has been studied extensively for its larger stimulated emission cross section and smaller fluorescence lifetime compared to other Nd doped crystals [7], [8]. Nd:YVO_4 is also capable of producing polarized laser radiation without any additional intra-cavity polarization dependent elements. Though the poor thermal mechanical properties of Nd:YVO_4 would result in spatial beam degradation and unexpected crystal fracture, operating with a lower pump power and/or controlling the doping concentration would reduce the thermal issues. However, further power scaling of Nd:YVO_4 lasers is still

Manuscript received 19 October 2022; accepted 20 October 2022. Date of publication 25 October 2022; date of current version 31 October 2022. This work was supported by the Ministry of Science and Technology (MOST), Taiwan under Grant MOST110-2221-E-035-056-MY2. *(Tin-Yu Yang and Yuan-Yao Lin are co-first authors.) (Corresponding authors: Shou-Tai Lin; An-Chung Chiang.)*

Tin-Yu Yang and Shou-Tai Lin are with the Department of Photonics, Feng Chia University, Taichung 407802, Taiwan (e-mail: j50831g1459@gmail.com; stailin@mail.fcu.edu.tw).

Yuan-Yao Lin is with the Department of Photonics, National Sun Yat-sen University, Kaohsiung 804201, Taiwan (e-mail: yuyalin@mail.nsysu.edu.tw).

An-Chung Chiang is with the Nuclear Science and Technology Development Center, National Tsing-Hua University, Hsinchu 300044, Taiwan (e-mail: acchiang@mx.nthu.edu.tw).

Digital Object Identifier 10.1109/JPHOT.2022.3216830

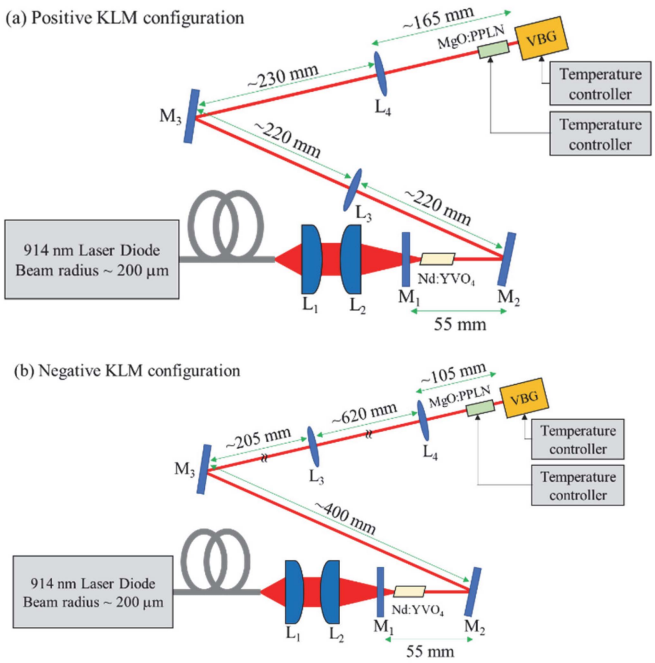

Fig. 1. Schematic setup of the cascaded mode-locked Nd:YVO_4 laser using MgO:PPLN with direct in-band diode pumping at 914 nm (not to scale). The ML cavity was formed by the mirrors M_1, M_2, M_3, and the volume Bragg grating, VBG. The positions of optical elements were properly adjusted for stable laser cavity modes for (a) positive KLM and (b) negative KLM. The distance between the MgO:PPLN crystal and the VBG was 3 mm.

limited. Direct in-band pump at 880 nm and 914 nm pumping has been demonstrated to be efficient for low-heat generation in Nd:YVO_4 lasers [9], [10]. It reduces the heat generation from every stimulated photon and significantly incurs lower thermal load inside the gain medium. The lower absorption at 914 nm permits the absorbed pump power to be more optimally distributed in a larger volume, thereby further reducing the thermal issues. This contributes to a better stability of the Nd:YVO_4 laser system and creates a possibility for laser power scaling with even better spatial beam quality.

In addition to the spatial beam quality, spectral control and stabilization are also important for mode-locked lasers. It has been demonstrated that the combination of a volume Bragg grating (VBG) and a quasi-phase-matching nonlinear medium provides spectral flexibility for CML [11]. In this paper, we report a cascaded mode-locked Nd:YVO_4 laser at 1064 nm with direct in-band pumping at 914 nm. A 25-mm-long MgO doped periodically-poled lithium niobate (MgO:PPLN) crystal was used to produce mode-locked laser pulses. A VBG was used to manipulate the output spectrum of the laser so as to stabilize the continues-wave mode locking (CWML).

II. Experimental Setup

Fig. 1 shows the schematic setup of the cascaded mode-locked Nd:YVO_4 laser at 1064 nm with direct in-band pumping at 914 nm. An a-cut, 20-mm-long, 1.5-at.% Nd doped YVO_4 crystal with an aperture of 4×4 mm^2 was used as the laser gain medium and polished with 1-degree wedge for avoiding the etalon effect. The Nd:YVO_4 crystal has anti-reflection (AR) coating ($R<1\%$) at 914 nm and 1064 nm. The Nd:YVO_4 was placed in a copper block for water cooling at 15 °C for heat dissipation. The pump laser was a 914-nm fiber-pigtailed laser diode with a 200-μm beam radius at its beam exit. The pump laser beam was focused into the Nd:YVO_4 crystal by a set of 25 mm:25 mm coupling lenses consisting of L_1 and L_2, as shown in Fig. 1. It was found that focusing the pump beam into the first third of the Nd:YVO_4 crystal yielded better performance of absorption.

The intra-cavity nonlinear optical crystal for mode locking was a 1-mm-thick, 25-mm-long, 5-mol.% doped MgO:PPLN crystal with a poling period of 6.92 μm which phase-matches 1064-nm second harmonic generation at 55.3 °C. The both end surfaces of the MgO:PPLN crystal have AR coatings at 532 nm and 1064 nm. If phase mismatching occurs in the intracavity nonlinear optical material, the sign of the nonlinear phase shift yields self-focusing (positive Kerr-lens/negative phase shift) or self-defocusing (negative Kerr-lens/positive phase shift) [12]. For a quasi-phase-matching nonlinear optical crystal, such as MgO:PPLN, temperature tunes the nonlinear phase shift. Effects of nonlinear phase in cascaded mode-locked Nd:YVO_4 laser have been discussed in our previous work [13]. In our experiment, the temperature of the MgO:PPLN crystal was set to be 47.5 °C and 62.5 °C for positive and negative KLM, respectively.

Intra-cavity lenses L_3 ($f = 250$ mm) and L_4 ($f = 125$ mm) were used to ensure a stable laser cavity mode in which the beam radius was $\sim$100 μm in the MgO:PPLN crystal and $\sim$300 μm in the Nd:YVO_4 crystal with thermal focal length upon suitable pump power and with proper positions of cavity components. The ML cavity was formed by the mirrors M_1, M_2, M_3, and the VBG (OptiGrate Inc.), which was 4.45 mm long and had an aperture of 8×6 mm^2. Its average reflectivity was $\sim$70% near a wavelength of 1064 nm, and the FWHM reflectivity bandwidth was 0.12 nm. Since the periodical structure of the VBG is affected by thermal expansion, changing the temperature of the VBG tunes the lasing wavelength.

III. Experimental Results and Discussions

A. Positive KLM Configuration

In the positive KLM configuration, the temperature of the MgO:PPLN crystal was set at 47.5 °C, being kept away from the phase-matching temperature 55.3 °C and resulting in negative nonlinear phase shift. The laser configuration is shown in Fig. 1(a) and the total length of the laser cavity was $\sim$900 mm. In the very beginning, we used an output coupler (OC) instead of the VBG. The OC was chosen to have partial reflectance ($\sim$78%) at 1064 nm and high reflectance (>99%) at 532 nm. It turned out that only Q-switched mode locking (QML) could be achieved. Fig. 2 shows typical temporal measurement of the QML pulses in the positive KML configuration using the OC while the 914 nm pump power was 48.9 W.

Being pumped by 912 nm, the pump absorption was weaker such that thermal focusing did not significantly contribute to the soft-aperture effect. Spatial mode matching becomes an important issue to the Q-switching stability limits of soft-aperture

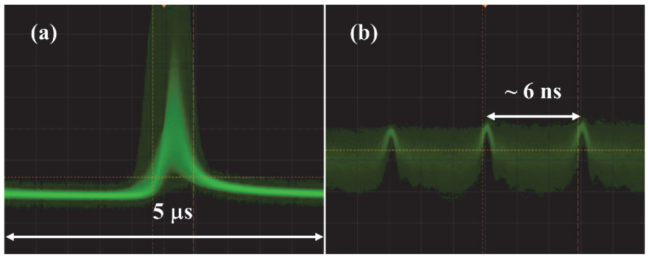

Fig. 2. A typical temporal profile of the QML pulses in the positive KML configuration using the OC. (a) Oscilloscope trace in 5-μs time span, (b) Oscilloscope trace in 20-ns time span.

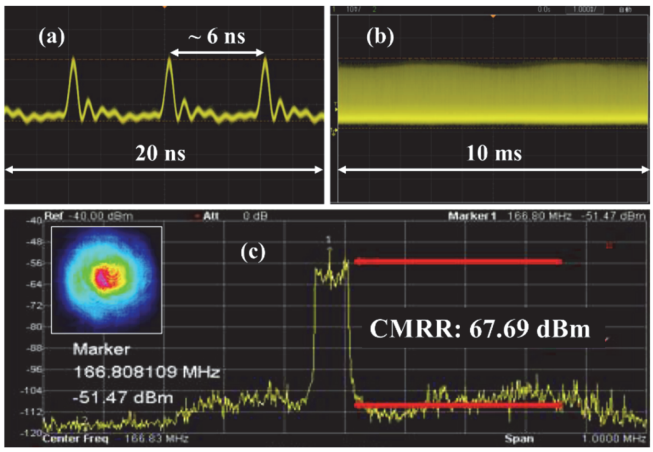

Fig. 3. A typical temporal profile of the CWML pulses in the positive KML configuration using the VBG. (a) Oscilloscope trace in 20-ns time span, (b) Oscilloscope trace in 10-ms time span, (c) Common-mode rejection ratio of the first beat mode. The inset of (c) shows the spatial profile of the CWML pulses.

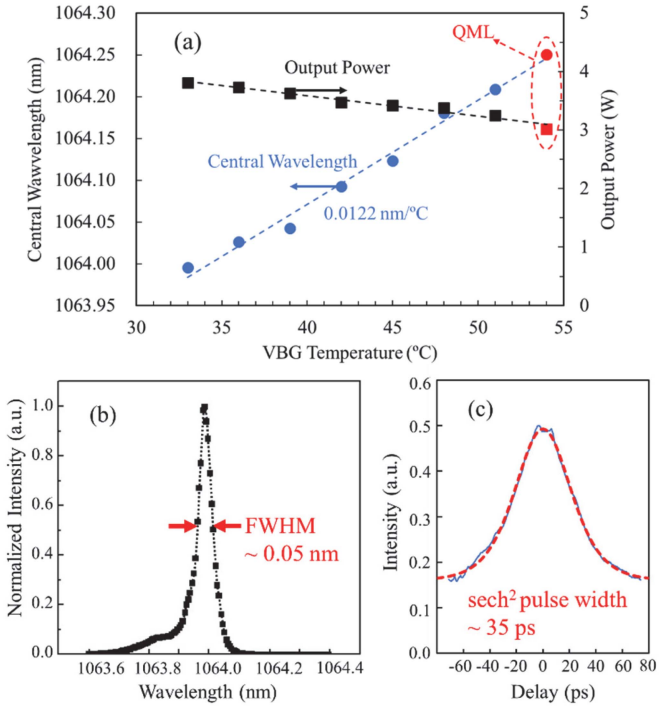

Fig. 4. (a) Central wavelength and output power as a function of VBG temperature. When the VBG temperature reached 54 °C, the CWML operation became QML. (b) A typical spectrum of the CWML pulses at 1064 nm. The FWHM spectral width is ~0.05 nm. (c) Autocorrelation measurement of the CWML pulse.

KLM [14]. In addition, the second harmonic fields reflected by the OC could affect the nonlinear amplitude and phase modulation over wavelength, the stability of mode-locking would be consequently affected. We replaced the OC with the VBG (operating at 33 °C) to provide spectral control so as to suppress the high-order spatial modes which contain additional spectral components. The oscillation frequency thus can be stabilized to provide continuous-wave mode locking (CWML). When the pump power was 59.2 W (30.8 W absorbed by the Nd:YVO_4 crystal), stabilized CWML was successfully achieved. The output power was 3.81 W.

The temporal characteristic of CWML was monitored by an oscilloscope (1-GHz bandwidth) and a RF spectrum analyzer (2-GHz bandwidth) with a fast photodiode (70-ps rise time). Fig. 3(a) and (b) show the oscilloscope signals with a time span of 20 ns and 10 ms, respectively, demonstrating pure CWML without QML background. The common-mode rejection ratio (CMRR) was found to be 67.69 dBm, which represents good stability of CWML, as shown in Fig. 3(c). The mode-locked repetition rate was found to be 166.8 MHz, which is consistent with the cavity length. The inset of Fig. 3(c) shows the spatial profile of the CWML pulses from the positive KLM configuration. The M^2 in the x-axis (horizontal) and the y-axis (vertical) were measured to be 1.79 and 1.06, respectively. We attribute that the inhomogeneous heat dissipating structure causes that the beam quality was worse in the horizontal direction.

As mentioned previously, the VBG temperature tunes the oscillation wavelength of the laser so as to alter the output power of the laser due to the wavelength dependent laser gain. Fig. 4(a) shows the central wavelength and output power as a function of VBG temperature. The output power decreased as the increasing VBG temperature and the oscillation wavelength. The wavelength tuning rate against VBG temperature was measured to be 0.0122 nm/°C, while the oscillation wavelength was 1064 nm at 33 °C. When the VBG temperature reached 54 °C, the oscillation wavelength was 1064.25 nm and the CWML operation became unstable and the QML pulses occurred. Fig. 4(b) shows a typical spectrum of the CWML pulses at 1064 nm and the full-width-at-half-maximum (FWHM) spectral width was ~0.05 nm. The autocorrelation trace was measured by an autocorrelator (APE pulseCheck USB 150) with a photodiode as the detector. The built-in filter function of the autocorrelator was used to obtain the integration of the photodetector over its response time so as to eliminate possible mechanical instabilities and obtain a better signal to noise ratio for the colinear intensity autocorrelation. Fig. 4(c) shows the autocorrelation trace (blue line) of the CWML pulses, and a fit (red dashed line), assuming $sech^2$-shaped pulses. Since the laser cavity was not thermally isolated or the pump power stabilized in any way, the autocorrelation trace shows some instability. While theoretical models for ideal ultra-fast lasers often predict $sech^2$ pulse shapes, the actual pulse duration can be determined from the FWHM width of the

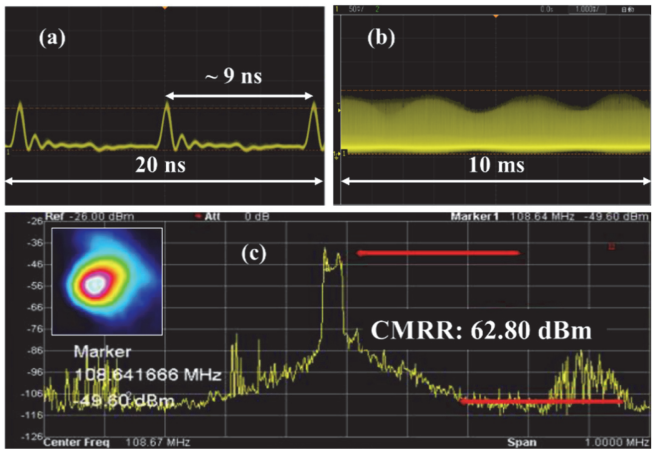

Fig. 5. A typical temporal profile of the CWML pulses in the negative KML configuration using the VBG. (a) Oscilloscope trace in 20-ns time span, (b) Oscilloscope trace in 10-ms time span, (c) Common-mode rejection ratio of the first beat mode. The inset of (c) shows the spatial profile of the CWML pulse.

fitted autocorrelation trace multiplied by 0.6482 [15]. Despite the instability, Fig. 4(c) shows a 54-ps autocorrelation width (FWHM), corresponding to a 35-ps pulse duration. The pulse energy was 23 nJ. The time-bandwidth product was calculated to be about 0.5. Without compensation of group velocity dispersion, a positively chirped pulse was expected. As the temperature was tuned, the pulse duration measured by the autocorrelator varied slightly with the laser resonant wavelengths and was within the range of 30 $\sim$ 35 ps.

B. Negative KLM Configuration

In the negative KLM configuration, we would like to demonstrate that the negative Kerr lens can account for the compensation of the excess of the thermal lens effect in the laser gain medium in which more pump power is absorbed. We intentionally increased the length of the laser cavity so that the laser cavity became unstable while thermal lensing effect was strong under high pump power. The laser configuration is shown in Fig. 1(b). Taking advantage of the effective negative lens contributed by the MgO:PPLN crystal at a specific temperature, it was possible to return the unstable laser cavity to a stable one. When the pump power was 62.5 W (32.5 W absorbed by the Nd:YVO_4 crystal) and the temperature of the MgO:PPLN crystal was 62.5 °C, stabilized CWML was successfully achieved. The output power was 4.81 W. Compared to the positive KLM configuration, the negative KLM configuration allowed more pump power and produced more output power.

Fig. 5(a) and (b) show the oscilloscope signals with a time span of 20 ns and 10 ms, respectively, demonstrating pure CWML without QML background. The CMRR was found to be 62.80 dBm, which represents good stability of CWML, as shown in Fig. 5(c). The mode-locked repetition rate was found to be 108.6 MHz, which is consistent with the cavity length. The inset of Fig. 5(c) shows the spatial profile of the CWML pulses from the negative KLM configuration. The M^2 in the x-axis (horizontal) and the y-axis (vertical) were measured to be 1.94 and 1.41, respectively. Again, we found the beam quality in the horizontal direction was worse than that in the vertical direction due to the inhomogeneous heat dissipation structure.

The temperature tuning of the VBG in the negative KLM configuration seemed to have similar behaviors as the positive KLM configuration, yielding small changes in the central wavelength and the output power. Despite the slower mode-locked repetition rate, the temporal profile of the negative KLM pulses is similar to the positive KLM one and their FWHM spectral widths are also similar. For the negative KLM configuration, the time-bandwidth product was $\sim$0.49 at 1064 nm.

C. Discussion on Instability of NLO Mode-Locking

In the laser cavity, the MgO:PPLN crystal, in addition to direct amplitude modulation, offers nonlinear phase modulation which turns to nonlinear loss modulation when combined with the soft aperture effect of finite sized pump beam in the gain medium. The loss modulation and nonlinear phase shifts can be estimated by the variation of resonator eigenmodes over linear eigenmodes of a laser cavity, which follows the equations 1 to 6 in [16]. Using the ABCD law for Gaussian beams [17], the laser beam radius in the laser cavity can be determined as shown in Fig. 6(a). We consider the configuration shown in Fig. 6(b) and take VBG as a resonator mirror that does not reflect second harmonic fields. The cavity fields at fundamental frequencies u_F and u_B in the forward and backward directions in the MgO:PPLN crystal generate second harmonic fields v_F and v_B, respectively. The nonlinear polarizations modulate the cavity fields at the fundamental frequencies. The normalized nonlinear amplitude modulation and normalized nonlinear phase shift can be determined for various phase mismatches ΔkL [13], [16] in the MgO:PPLN crystal. These phase mismatches correspond to the resonating fundamental wavelengths by employing the extended Sellmeier equation revealed in 2017 [18].

Fig. 6(c) shows the calculated normalized nonlinear transmission and normalized phase shift as a function of ΔkL in the 25-mm-long MgO:PPLN crystal placed in the laser cavity of the positive KML configuration illustrated in Fig. 1(a). The intracavity laser power adopted is 10 W when the output coupling is 30%. Particular normalized nonlinear transmission as a function of frequency detuning and accumulated phase mismatches are calculated at 52.75 °C. The theoretical calculation illustrates positive nonlinear phase shift within a frequency range of approximately 0.1 nm, which can be totally covered by the reflection band ($\sim$0.12 nm) of the VBG used in our experiment. In contrast, with an OC that highly reflects second harmonic fields back to the MgO:PPLN crystal, the interference of second harmonic fields produces severe oscillation and dispersion to the nonlinear amplitude and phase modulation over wavelength and consequently leads to instability of mode locking. In our experiment, the corresponding ΔkL at 47.5 °C is about 15π, which is beyond the strongly oscillated region shown in Fig. 6(c). The reflected SHG fields would not affect the stability of CWML.

Moreover, as the pump power increases, thermal lensing occurs to affect the laser stability and mode-locking behavior [19] when mode-locked lasers are often designed near the stability

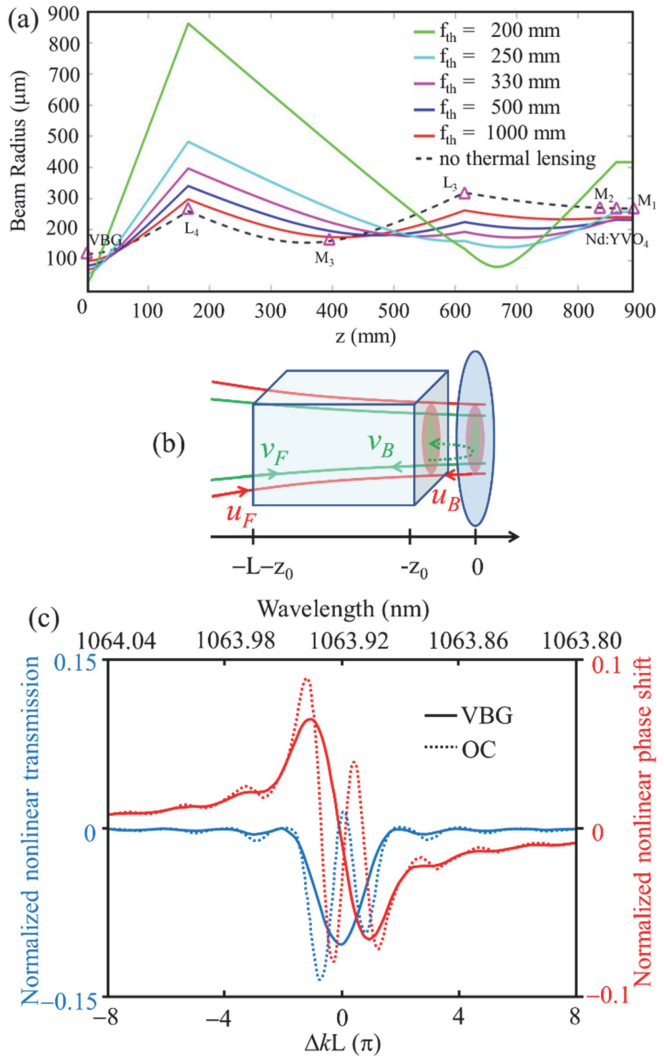

Fig. 6. (a) Calculated transverse beam radius of laser intensity in the resonator of the positive KML configuration illustrated in Fig. 1(a). The fundamental wave and the second harmonic field near the MgO: PPLN crystal and OC/VBG are illustrated in (b) and are used to estimate the normalized nonlinear transmission and normalized nonlinear phase shift in the MgO:PPLN crystal revealed in (c). $z_0 = 5$ mm and L = 25 mm indicate the location of the MgO:PPLN crystal from the OC/VBG.

border. We calculated the variation of laser beam radius under the influence of thermal lensing effect in the laser gain medium. While the effective thermal induced focal length is greater than 250 mm, little variation in the beam radius on VBG/OC is perceived. In particular the normalized nonlinear amplitude modulation and normalized nonlinear phase shift increases as the beam radius in the MgO:PPLN crystal gradually drops given a shorter effective thermal induced focal length with higher pump power. However, when the effective thermal induced focal length drops to 200 mm, significant increase in the beam radius near the VBG/OC is calculated. It causes severe modal mismatch between the pump laser beam and the resonating modes inside the laser gain material. In addition, the laser cavity no longer supports a stable laser mode if the thermal focal length is shorter than 200 mm in the positive KLM configuration. The laser obviously becomes unstable under high pump power. The

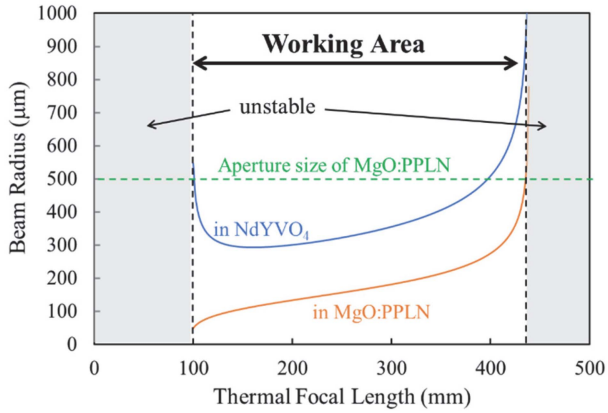

Fig. 7. Calculated beam radii in NdYVO$_4$ and in MgO:PPLN for the negative KML configuration illustrated in Fig. 1(b). The grey areas denote unstable laser cavities. The aperture size of MgO:PPLN also slightly limits the working area.

in-band pump by 914 nm that produces less thermal lensing effect in Nd:YVO$_4$ by a factor of 2.1 [20] potentially improves the stability of mode-locking operation.

The negative KLM configuration introduces a negative Kerr focal length which would compensate the strong thermal lensing effect under high power pumping scheme, permitting more pump power into Nd:YVO$_4$. Fig. 7 shows the beam radii in Nd:YVO$_4$ and MgO:PPLN as a function of thermal focal length for the negative KML configuration shown in Fig. 1(b). It is found that in the negative KLM configuration, the thermal focal length can be further reduced to 100 mm and the laser cavity still remains stable. Consequently, the output power is significantly higher than that of the positive KLM configuration. However, the cavity stability for the negative KLM configuration only occurs when the effective thermal focal length ranges from 100 mm to 430 mm. The negative KLM configuration requires thermal lensing to maintain the cavity stability and would not be operable with lower pump power. As can be seen from Fig. 7, a possible working area is found by considering the stability condition of the resonator and the aperture size of the MgO:PPLN crystal. Also, the calculation shows a ∼300-μm beam radius in the Nd:YVO$_4$ crystal which does not match the 200-μm pump beam radius. Unless we replace the input coupler, the mode-overlapping could not be optimized for better performance. In addition, the current negative KLM configuration is only simple modification of the positive one. The "lower arm" of the z-folded laser cavity remains unchanged for the ease of measuring the absorbed pump power.

The poor stability of the negative KLM configuration can also be attributed to the disturbance of air and temperature. The current system does not have thermal shielding for the MgO:PPLN crystal due to the limited space near the VBG. Even if the temperature is controlled within ±0.1 °C, tiny disturbance will still significantly affect the stability while the negative KLM is operated near the unstable region.

D. Pulse Duration and Bandwidth

The bandwidth of the laser system is limited by the volume Bragg grating (VBG). In [11], they used a VBG with a FWHM

linewidth (bandwidth) of 0.32 nm (90.6 GHz@1029 nm) and obtained a 24-GHz mode-locked bandwidth during which the VBG has the highest reflectivity. The actual mode-locked bandwidth was further reduced due to the sinc-shape reflection spectrum of the VBG. In our case, we used a VBG with a FWHM spectral width of 0.12 nm (31.8 GHz@1064 nm) and measured a ∼13-GHz (0.05 nm) mode-locked bandwidth while the sech^2 pulse duration was measured to be within the range of $30 \sim 35$ ps. The time bandwidth product is 1.5 times that of the Fourier limit despite some measurement errors; the 0.05-nm spectral width was roughly determined from the FWHM width of the laser spectrum and might have small deviation. If a VBG with a broader bandwidth can be used, the pulse duration could be further reduced. On the other hand, in the process of cascade $\chi^{(2)}$, group velocity mismatch (GVM) between the fundamental wave (1064 nm) and the second harmonic wave (532 nm) in the nonlinear crystal, expressed by

$$\text{GVM} = \frac{1}{\text{v}_{\text{g},532}} - \frac{1}{\text{v}_{\text{g},1064}}, \tag{2}$$

where $\text{v}_{\text{g},\#}$ are group velocities of wavelengths #, plays an important role. Without the limitation of the VBG bandwidth, the shortest pulse duration can be determined by the GVM multiplied by 2 times of the SHG coherent length for phase-mismatched NLM mode locking [13]. For the MgO:PPLN crystal (GVM $\sim$ 0.5 ps/mm with refractive index obtained by [18]) used in our experiment, the shortest pulse duration is calculated to be 1.8 ps while ΔkL is 15π.

IV. Conclusion

In conclusion, we have demonstrated cascaded mode-locked Nd:YVO_4 laser at 1064 nm with direct in-band pumping at 914 nm. A 25-mm-long MgO:PPLN crystal was used to produce mode-locked laser pulses. For 914 nm pumping, the thermal lensing effect was smaller and the soft aperture effect became weaker. Large power throughput was allowed by the reduced thermal lensing effect with pumping at 914 nm. With the OC, backward second harmonic fields would affect nonlinear amplitude modulation and phase shift within a small range near the phase-matching point of the MgO:PPLN crystal. The VBG helped to provide spectral control in output spectrum, resulting in successful CWML within the VBG bandwidth. Wavelength tuning was achieved by altering the temperature of the VBG.

In optimizing the performance of the mode-locked laser, there is trade-off between thermal focusing, nonlinear amplitude modulation, nonlinear phase shift, cavity design, mode matching, etc. Some of these parameters are related to each other. A systematic way of optimization might need to be developed.

References

[1] D. E. Spence, P. N. Kean, and W. Sibbett, "60-fsec pulse generation from a self-mode-locked ti:Sapphire laser," *Opt. Lett.*, vol. 16, no. 1, pp. 42–44, Jan. 1991, doi: 10.1364/OL.16.000042.

[2] M. Piché and F. Salin, "Self-mode locking of solid-state lasers without apertures," *Opt. Lett.*, vol. 18, no. 13, pp. 1041–1043, Jul. 1993, doi: 10.1364/OL.18.001041.

[3] K. A. Stankov and J. Jethwa, "A new mode-locking technique using a nonlinear mirror," *Opt. Commun.*, vol. 66, no. 1, pp. 41–46, Apr. 1988, doi: 10.1016/0030-4018(88)90201-5.

[4] R. DeSalvo, D. J. Hagan, M. Sheik-Bahae, G. Stegeman, E. W. Van Stryland, and H. Vanherzeele, "Self-focusing and self-defocusing by cascaded second-order effects in KTP," *Opt. Lett.*, vol. 17, no. 1, pp. 28–30, Jan. 1992, doi: 10.1364/OL.17.000028.

[5] G. I. Stegeman, D.J. Hagan, and L. Torner, "$\chi(2)$ cascading phenomena and their applications to all-optical signal processing, mode-locking, pulse compression and solitons," *Opt. Quantum Electron.*, vol. 28, pp. 1691–1740, Dec. 1996, doi: 10.1007/BF00698538.

[6] S. Mukhopadhyay, "Picosecond optical pulse generation by nonlinear mirror mode-locking: A review," *Indian J. Sci. Technol.*, vol. 10, no. 28, pp. 1–11, Jul. 2017, doi: 10.17485/ijst/2017/v10i28/115689.

[7] W. Koechner, "Properties of solid-state laser materials," in *Solid-State Laser Engineering*, 6th ed. New York, NY, USA: Springer, 2006, pp. 38–101.

[8] A. W. Tucker, M. Birnbaum, C. L. Fincher, and J. W. Erler, "Stimulated emmision cross section at 1064nm and 1342nm in Nd:YVO4," *J. Appl. Phys.*, vol. 48, no. 12, pp. 4907–4911, Dec. 1977, doi: 10.1063/1.323618.

[9] L. McDonagh, R. Wallenstein, R. Knappe, and A. Nebel, "High-efficiency 60 W TEM00 nd:YvO_4 oscillator pumped at 888 nm," *Opt. Lett.*, vol. 31, no. 22, pp. 3297–3299, Nov. 2006, doi: 10.1364/OL.31.003297.

[10] D. Sangla, M. Castaing, F. Balembois, and P. Georges, "Highly efficient Nd:YvO_4 laser by direct in-band diode pumping at 914 nm," *Opt. Lett.*, vol. 34, no. 14, pp. 2159–2161, Jul. 2009, doi: 10.1364/OL.34.002159.

[11] N. Meiser, K. Seger, V. Pasiskevicius, A. Zukauskas, C. Canalias, and F. Laurell, "Cascaded mode-locking of a spectrally controlled Yb:KYW laser," *Appl. Phys. B*, vol. 116, no. 2, pp. 493–499, Aug. 2014, doi: 10.1007/s00340-013-5725-6.

[12] R. DeSalvo, D. J. Hagan, M. Sheik-Bahae, G. Stegeman, E. W. Van Stryland, and H. Vanherzeele, "Self-focusing and self-defocusing by cascaded second-order effects in KTP," *Opt. Lett.*, vol. 17, no. 1, pp. 28–30, Jan. 1992, doi: 10.1364/OL.17.000028.

[13] S. T. Lin and C. H. Huang, "Effects of nonlinear phase in cascaded mode-locked Nd:YvO_4 laser," *Opt. Exp.*, vol. 27, no. 2, pp. 504–511, Jan. 2019, doi: 10.1364/OE.27.000504.

[14] S. Kimura, S. Tani, and Y. Kobayashi, "Q-switching stability limits of Kerr-lens mode locking," *Phys. Rev. A*, vol. 102, no. 4, Oct. 2020, Art. no. 043505, doi: 10.1103/PhysRevA.102.043505.

[15] K. L. Sala, G. A. Kenny-Wallace, and G. E. Hall, "CW autocorrelation measurements of picosecond laser pulses," *IEEE J. Quantum Electron.*, vol. 16, no. 9, pp. 990–996, Sep. 1980, doi: 10.1109/JQE.1980.1070606.

[16] M. Zavelani-Rossi, G. Cerullo, and V. Magni, "Mode locking by cascading of second-order nonlinearities," *IEEE J. Quantum Electron.*, vol. 34, no. 1, pp. 61–70, Jan. 1998, doi: 10.1109/3.655008.

[17] B. E. A. Saleh and M. C. Teich, "Beam optics," in *Fundamental of Photonics*. New York, NY, USA: Wiley, 1991, pp. 80–107.

[18] H. B. Lin et al., "Extended sellmeier equation for the extraordinary refractive index of 5% mgo-doped congruent linbo3 at high temperature," *AIP Adv.*, vol. 7, no. 9, Sep. 2017, Art. no. 095201, doi: 10.1063/1.4994104.

[19] X. G. Huang, W. K. Lee, S. P. Wong, J. Y. Zhou, and Z. X. Yu, "Effects of thermal lensing on stability and astigmatic compensation of a Z-fold laser cavity," *J. Opt. Soc. Amer. B*, vol. 13, no. 12, pp. 2863–2869, Dec. 1996, doi: 10.1364/JOSAB.13.002863.

[20] T. Waritanant and A. Major, "Thermal lensing in nd:YVO4 laser with in-band pumping at 914 nm," *Appl. Phys. B*, vol. 122, no. 5, May 2016, Art. no. 135, doi: 10.1007/s00340-016-6417-9.